Electronic Supplementary Material (ESI) for New Journal of Chemistry.

Electronic Supplementary Information (ESI)

Post-Synthesis Modification of Functionalised Polyhedral Oligomeric Silsesquioxanes with Encapsulated Fluoride – Enhancing Reactivity of T_8-F POSS for Materials Synthesis

Mathilde Laird,[a] Philippe Gaveau,[a] Philippe Trens,[a] Carole Carcel,[a] Masafumi Unno,[b] John R. Bartlett,*[c] and Michel Wong Chi Man*[a]

[a] *ICGM, Univ Montpellier, CNRS, ENSCM, Montpellier, France.*

[b] *Department of Chemistry and Chemical Biology, Graduate School of Science and Technology, Gunma University, Kiryu 376-8515, Gunma, Japan.*

[c] *Western Sydney University, Locked Bag 1797 Penrith NSW 2751 Australia.*

**Corresponding Authors: j.bartlett@westernsydney.edu.au; Michel.wong-chi-man@enscm.fr*

Table of Contents

1. Results and Discussion

1.1 Heck coupling reaction

Following [1], styryl-functionalised T_8-F (50.0 mg, 33.2 µg, 1 eq) and tetrakis(triphenylphosphine)palladium(0) (15.4 mg, 13 µmol, 0.05 eq per styryl) were added to a flame-dried rotaflow® flask, under an inert atmosphere. The solids were dissolved in distilled DMF (1.0 mL) followed by addition of dicyclohexylmethylamine (70 µL, 299 µmol, 9 eq) and iodobenzene (35 µL, 292 µmol, 1.1 eq per styryl). The reaction mixture was subsequently held overnight at 120 °C under homogeneous agitation. The solvent was then evaporated, and the crude reaction product analysed by ^{1}H solid state NMR spectroscopy.

As shown in Fig. S1 (bottom), the spectrum exhibits broad signals and multiplets arising from degradation of the T_8-F moiety. The absence of the expected vinyl signals in the spectrum of the crude product is unexpected, further confirming that the Heck coupling reaction has not yielded the desired products. The reaction was also attempted using dioxane as a solvent and with bromobenzene as reactant; as above, degradation of the T_8-F moiety was observed.

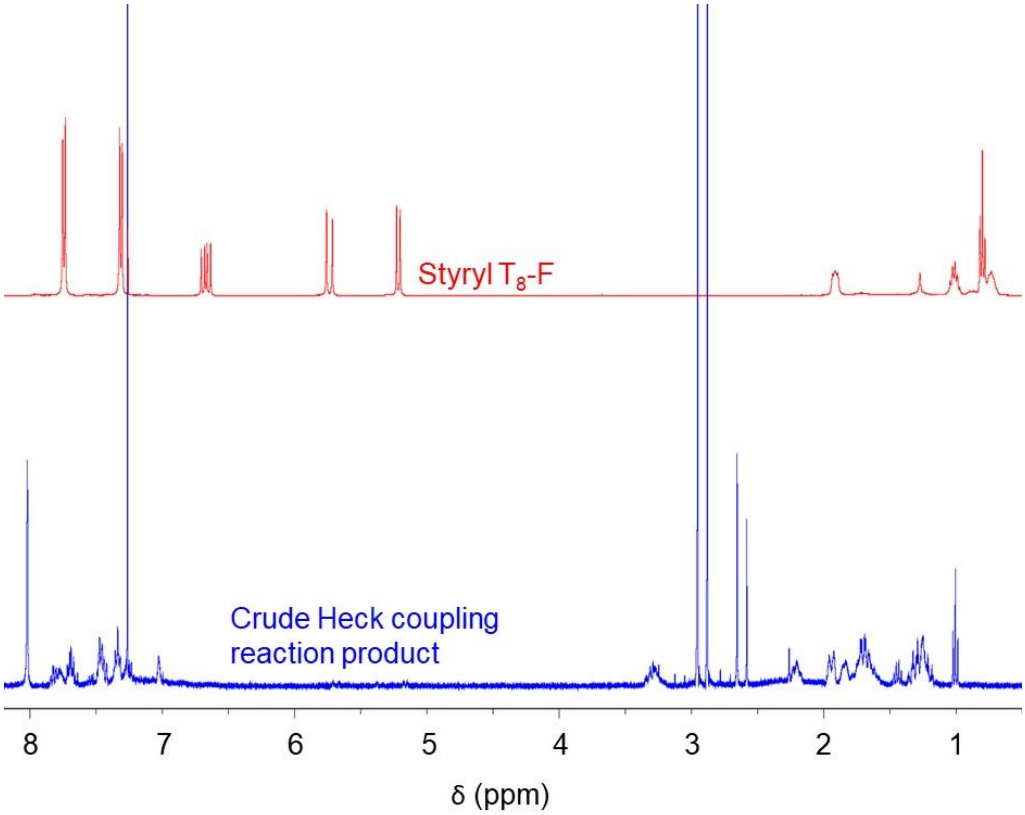

Fig. S1. Solution ^{1}H NMR spectra of styryl T_8-F (top [2]) and the crude Heck coupling reaction product (bottom).

1.2 Hydrosilylation reaction

Following [3-6], a solution of styryl-functionalised T_8-F (50.0 mg, 33.2 µg, 1 eq) in dry THF was prepared under an inert atmosphere in a flame-dried rotaflow® flask. Trimethoxysilane (50 µL, 399 mmol, 1.5 eq per styryl) was added, followed by addition of Karstedt's catalyst (10 % Pt in *i*-Pr; 50 µL, 2.65 µmol, 1 mol % Pt) at 0 °C. The reaction was held overnight at room temperature under homogeneous agitation. The solvent was then evaporated, and the crude reaction product analysed by ^{1}H, ^{19}F and ^{29}Si.

The ^{1}H NMR spectrum of the reaction product (Fig. S2, bottom) confirms that the reaction has gone to completion, through the loss of the signals associated with the vinylic protons of the styryl-functionalised T_8-F precursor at 6.7, 5.7 and 5.2 ppm (Fig. S2, top). However, a variety of broad signals are observed in the spectrum of the product (Fig. S2, bottom), consistent with degradation of the T_8-F cage. In addition, the ^{29}Si NMR spectrum shows multiple signals (Fig. S3, bottom), instead of the expected sharp signal associated with the T_8-F cage (Fig. S3, top) and additional resonances arising from the trimethoxysilyl substituent. In particular, the loss of the signal associated with the T_8-F cage at around -81 ppm, together with the appearance of two signals at around -78 ppm attributable to fluoride-free styryl-functionalised T_8 cages [7] are entirely consistent with degradation of the T_8-F moiety. Finally, the ^{19}F NMR spectrum of the hydrosilylation product (not shown) exhibits a signal at -25 ppm arising from the T_8-F moiety, together with multiple signals between -130 and -140 ppm attributed to T_8-F cage-degradation products.

Finally, the hydrosilylation reaction was repeated using trichlorosilane instead of trimethoxysilane, with similar results.

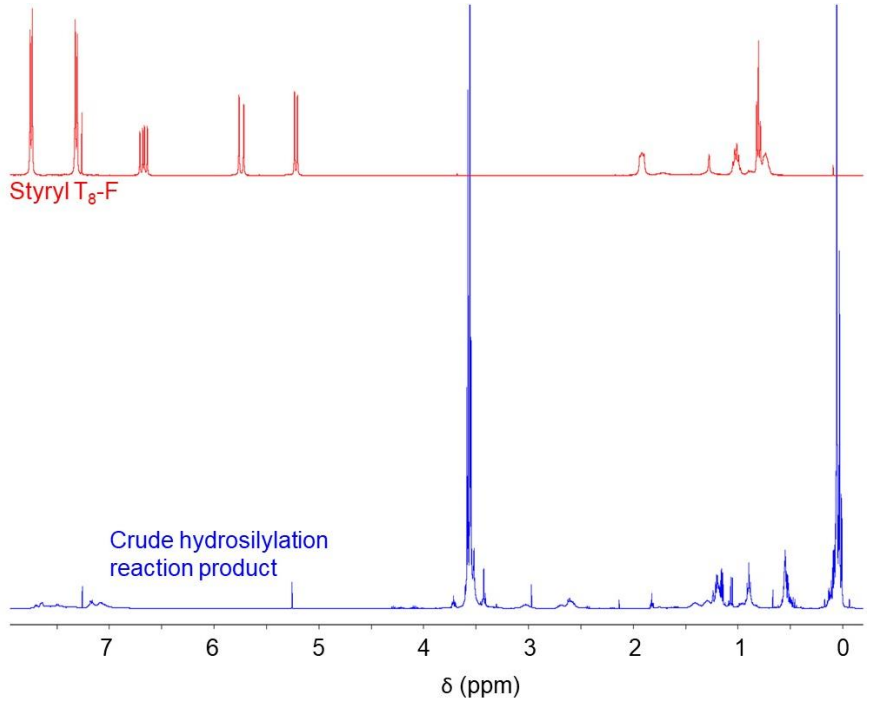

Fig. S2. ^{1}H NMR spectra of styryl T_8-F (top [2]) and the crude hydrosilylation reaction product (bottom).

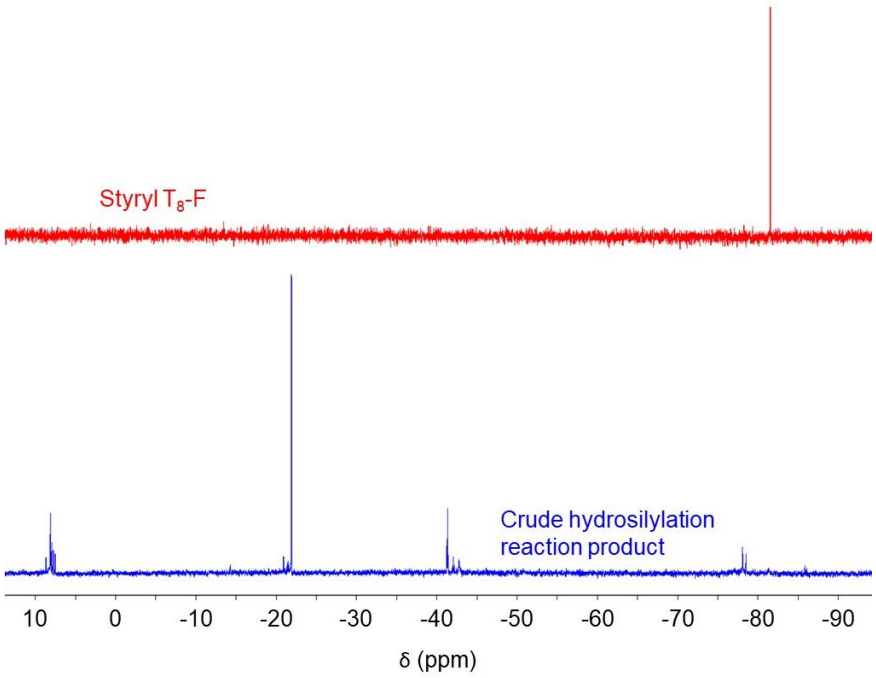

Fig. S3. ^{29}Si NMR spectra of styryl T_8-F (top [2]) and the crude hydrosilylation reaction product (bottom).

1.3 Metathesis reaction

Following [8], styryl-functionalised T_8-F (50.6 mg, 33.2 µmol, 1 eq) was added to a flame-dried rotaflow® flask under an inert atmosphere. The solid was dissolved in dry chloroform (1.0 mL), followed by addition of styrene (70 µL, 610 µmol, 2.3 eq per styryl) and Grubbs 1st generation catalyst (4.1 mg, 5 µmol, 0.02 eq per styryl). The mixture was frozen and placed under vacuum for outgassing. The reaction mixture was subsequently held overnight at 80 °C under homogeneous agitation in a closed vessel. The solvent was then evaporated, and

the crude reaction product analysed by ^{1}H, ^{19}F and ^{29}Si NMR.

The completion of the cross-metathesis reaction is demonstrated by the loss of the characteristic vinyl signals of the styryl-functionalised T_8-F precursor in the ^{1}H NMR spectrum at 6.7, 5.7 and 5.2 ppm (Fig. S4, top) and the appearance of new vinylic signals at 5.7 and 5.0 ppm in the spectrum of the product (Fig. S4, bottom). However, the presence of broad signals at around 7-8 ppm in the latter spectrum is consistent with degradation of the cage.

The ^{19}F NMR spectrum of the product (not shown) exhibits relatively broad signals at -25.3, -133.0 and -146.6 ppm, which are attributed to a mixture of products and TBAF [9]. The latter is indicative of the formation of fluorinated by-products arising from degradation of the T_8-F cage and associated release of fluoride.

The ^{29}Si NMR spectrum of the styryl-functionalised T_8-F precursor (Fig. S5, top) exhibits the expected single sharp signal at around -81 ppm arising from the T_8-F cage [2]. However, the spectrum of the metathesis reaction product exhibits two sharp signals at -54.4 ppm, with only weak, broad features observed near -81 ppm (Fig. S5, bottom). The loss of the signal near -81 ppm is consistent with degradation of the T_8-F cage, while the two sharp signals at -54.4 ppm are attributed to degradation products such as aryl-functionalised T^1 and T^0 species. For example, Ph-Si$(OH)_3$ exhibits a ^{29}Si NMR signal at -49.3 ppm [10], arising from the T^0 silicon site.

The metathesis reaction was also attempted using other substrates, including octene, naphthalene and styryltrimethoxysilane, with similar results to those obtained with styrene. The reactions were also conducted at ambient temperature and 50 °C, and under strictly stoichiometric conditions. In all cases, degradation of the T_8-F moiety was observed.

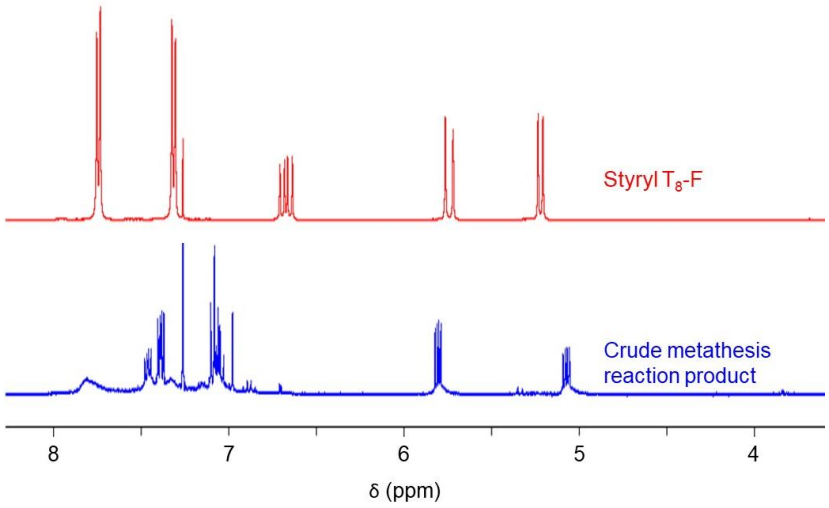

Fig. S4 Solution ^{1}H NMR spectra of styryl T_8-F (top [2]) and the crude metathesis reaction product (bottom).

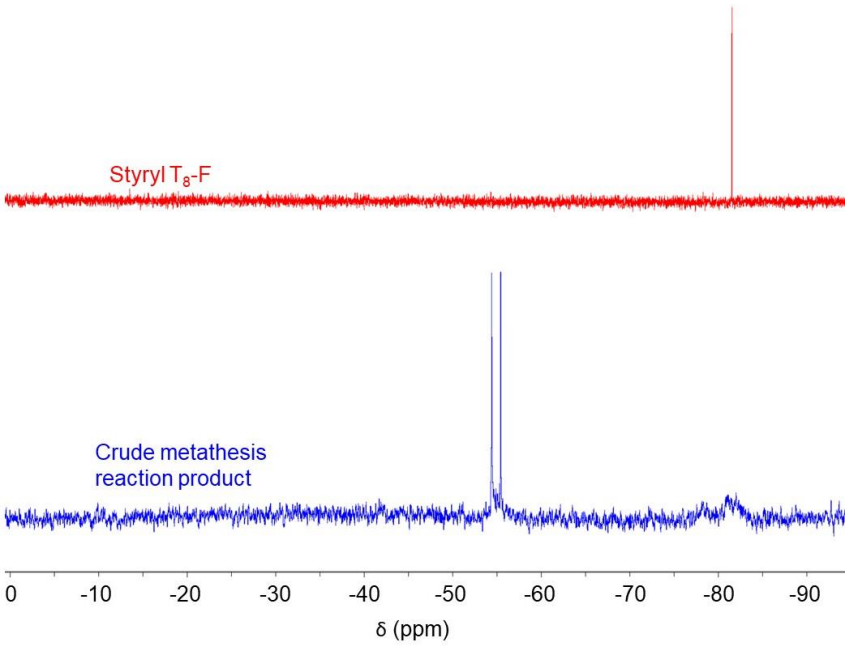

Fig. S5 Solution ^{29}Si NMR spectra of styryl T_8-F (top [2]) and the crude metathesis reaction product (bottom).

1.4 Functionalisation of octastyryl T_8-F

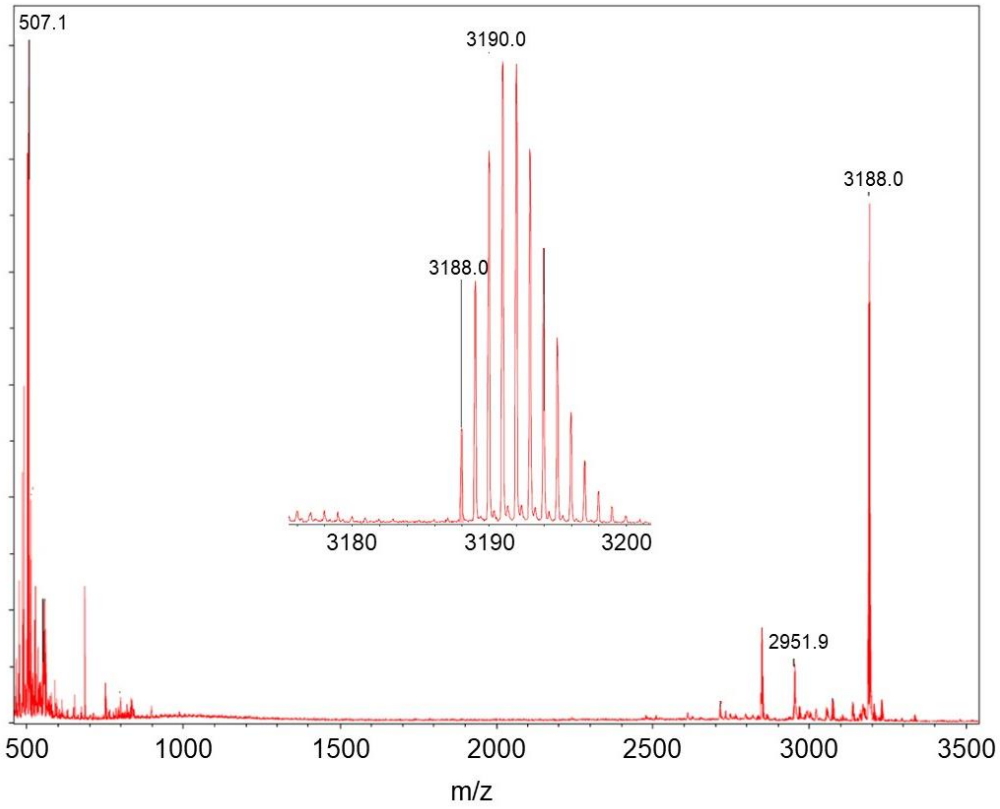

Fig. S6. MALDI-TOF mass spectrum of the triethoxysilylated functionalised T_8-F cage.

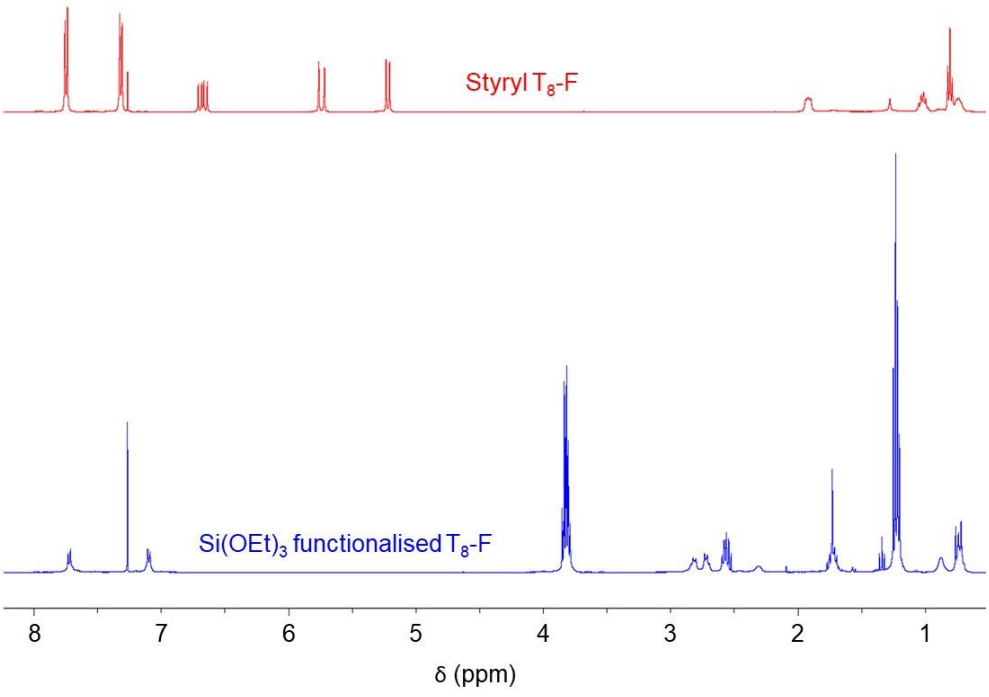

Fig. S7. Solution ^{1}H NMR spectra of the styryl- (top [2]) and triethoxysilylated functionalised T_8-F cages (bottom).

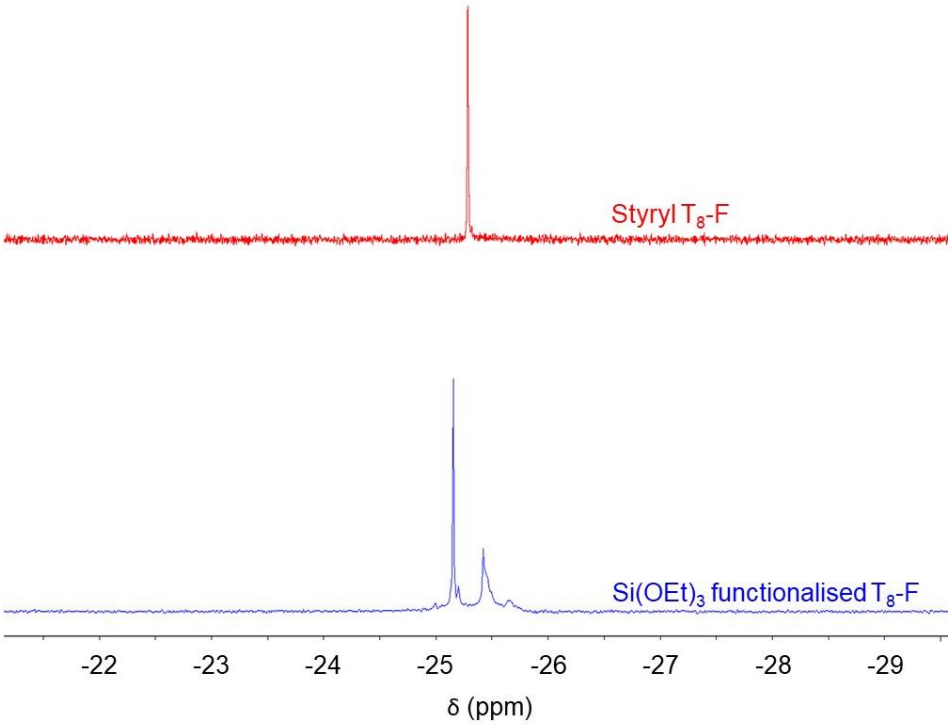

Fig. S8. Solution ^{19}F NMR spectra of the styryl- (top [2]) and triethoxysilylated functionalised T_8-F cages (bottom).

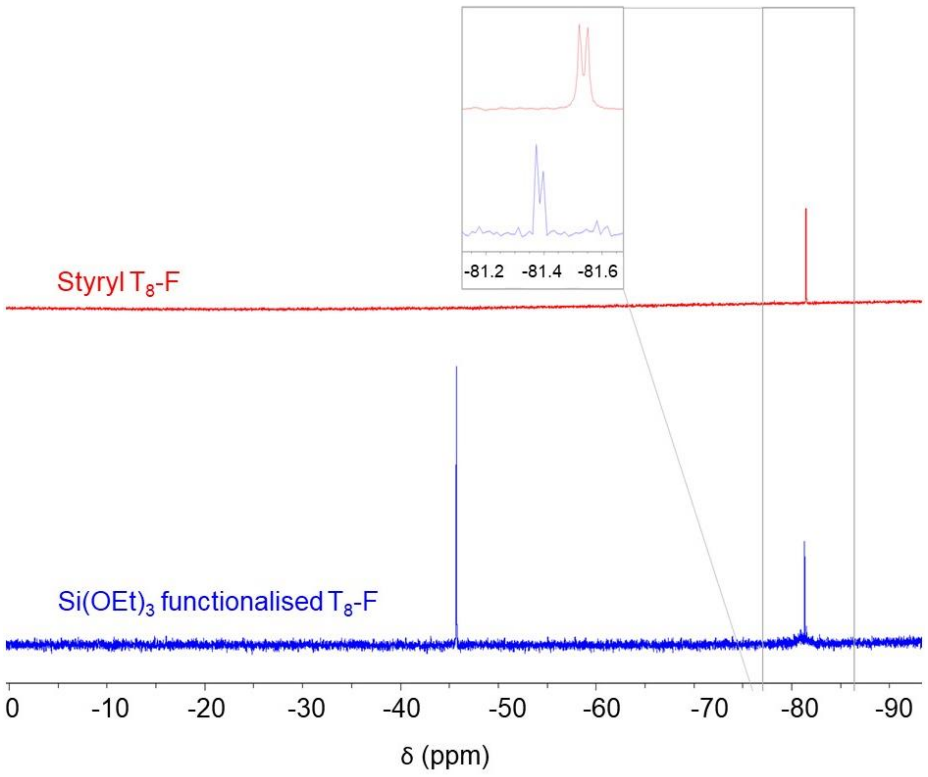

Fig. S9. Solution ^{29}Si NMR spectra of the styryl- (top [2]) and triethoxysilylated functionalised T_8-F cages (bottom).

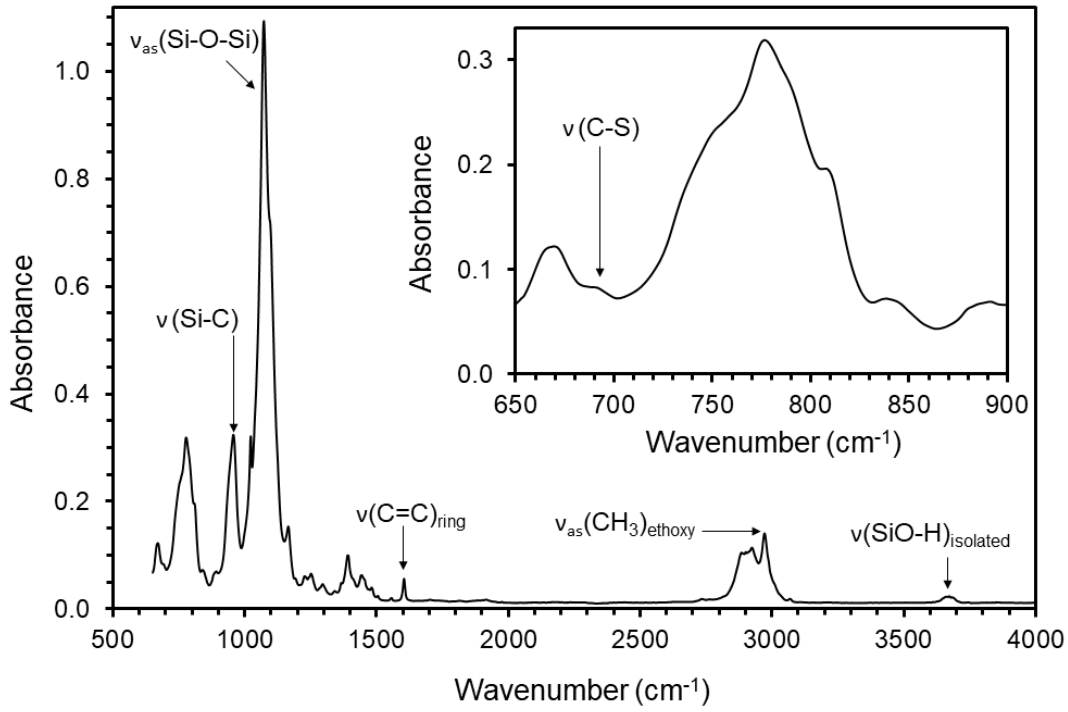

Fig. S10. FTIR spectrum of the triethoxysilylated functionalised T_8-F precursor.

1.5 Identification of minor by-products observed during the AIBN-catalysed thiol-ene click reaction

As indicated in Section 3.1 (main document), the ^{19}F and ^{29}Si liquid NMR spectra of the product obtained from the thiol-ene click reaction between styryl-functionalised T_8-F and 3-thiopropyltriethoxysilane exhibit signals expected from the desired triethoxysilylated T_8-F compound, together with additional signals attributed to a minor product. Here, we discuss the approaches taken by us to establish the composition of this minor product.

Bassindale and co-workers have reported the ^{19}F and ^{29}Si chemical shifts of X-C_6H_4-functionalised T_8-F compounds for a range of different X substituents [11], which were all recorded under identical conditions (and hence constitute a robust, internally-consistent data set in which the impact of X on the chemical shift might be assessed). These are summarised in Table S1, together with the electron-withdrawing "strength" of the X-C_6H_4- moieties at the para carbon, based on molecular electrostatic potential (MESP) analyses by Remya and Suresh [12]. Here, positive values of ΔV_C (with respect to the MESP values for phenyl) correspond to substituents which are more strongly electron-withdrawing than phenyl, while negative values correspond to substituents which are less electron withdrawing (or more electron donating) than phenyl. It is immediately evident that there is no robust correlation between ΔV_C across a wide range of values (from -5.0 to 7.6 kcal/mol) and the observed chemical shifts (e.g., from -25.2 to -27.2 ppm for the ^{19}F signals). This immediately suggests that the relatively small upfield shifts observed in our work (from -25.2 ppm for the major product to -25.4 ppm for the minor product) cannot be reliably interpreted simply on the basis of electronic effects.

We next consider possible ring strain arguments, with the data of Bassindale and co-workers again providing a robust, internally-consistent dataset for exploring potential structure correlations with variations in ^{29}Si chemical shifts, as summarised in Table S2. It should be noted that our data were obtained under different conditions than those used in [11], and hence, we focus on variations in chemical shift with changing functional group and T_8-F geometry rather than the magnitudes of the chemical shifts themselves. We also note that the structural parameters summarised in Table S2 were obtained from solid samples, while the corresponding chemical shifts were recorded from samples in solution, where different molecular geometries may be possible. In the case of the data presented in [11], it is evident that changes in average Si-O-Si bond angle of less than 0.4 ° (which are modulated by the respective functional group) lead to a corresponding change of less than 0.5 ppm in the ^{29}Si chemical shift. The other structural parameters for the compounds in [11] vary by even smaller amounts. Further, the variations in chemical shift in our system are significantly less than those reported in [11], suggesting that it is not appropriate to invoke ring strain arguments to account for the small variations in ^{29}Si chemical shift observed in our work. Finally, as previously reported by us [13], the solution ^{29}Si chemical shift arising from the 5^24^1 cages in styryl-functionalised T_{18}, T_{12} and T_{10} POSS only vary by around 0.2 ppm across this family of compounds (-79.35, -79.45 and -79.59 ppm, respectively), further illustrating the issues associated with using POSS ring strain arguments to interpret such small variations in chemical shift.

Table S1 Solution $^{19}F/^{29}Si$ NMR chemical shifts of selected organo-functionalised T_8-F compounds and corresponding MESP values of functional groups

Aryl Functional Group	ΔV_C (kcal/mol)	Chemical shift / ppm		Comments
		^{19}F	^{29}Si	
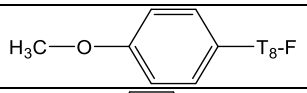	-5.0	-27.6	-80.2	Ref. [11]
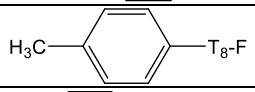	-3.3	-26.8	-80.4	Ref. [11]
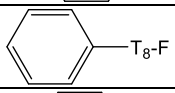	0.0	-26.4	-80.6	Ref. [11]
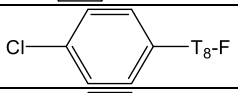	7.0	-27.2	-80.7	Ref. [11]
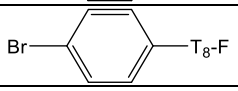	7.6	-27.2	-80.5	Ref. [11]
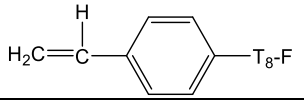	1.0	-25.2	-81.5	This work: styryl-functionalised T_8
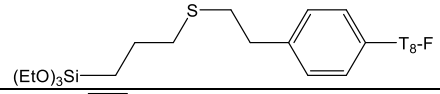	-	-25.2	-81.4	This work: thiol-ene click product
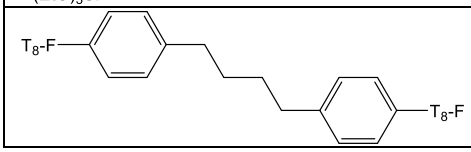	-3.1 to -3.3 [§]	-25.4	-81.6	This work: proposed dimer

[§] Based on the values for $-CH_2CH_2C_6H_5$ (-3.1); $-CH_2CH_2CH_3$ (-3.1); $-(CH_2)_3CH_3$ (-3.2); $-(CH_2)_4CH_3$ (-3.2); $-(CH_2)_6CH_3$ (-3.2)

Table S2 Solution ^{29}Si NMR chemical shifts of selected organo-functionalised T_8-F compounds and corresponding geometrical parameters (determined via single-crystal XRD)

Aryl Functional Group	Bond lengths/distances / Å				Bond angles / °		^{29}Si shift / ppm	Comments
	Si…F	Si-C	Trans Si…Si	Si-O	O-Si-O	Si-O-Si		
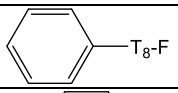	2.65	1.86	5.31	1.62	112.8	141.2	-80.6	Ref. [11]
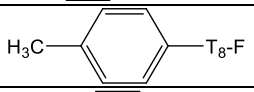	2.66	1.86	5.31	1.63	112.8	141.2	-80.4	Ref. [11]
	2.65	1.85	5.30	1.62	112.9	141.0	-80.7	Ref. [11]
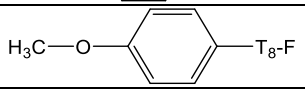	2.66	1.86	5.32	1.63	112.7	141.4	-80.2	Ref. [11]
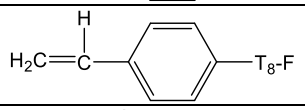	2.65	1.83	5.30	1.62	112.6	141.6	-81.5	This work: styryl-functionalised T_8
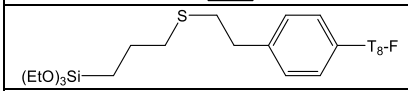	-	-	-	-	-	-	-81.4	This work: thiol-ene click product
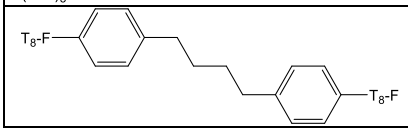	-	-	-	-	-	-	-81.6	This work: proposed dimer

We also considered the possibility that the minor products might arise from partial hydrolysis of the ethoxy ligands. However, these are located more than 10 atoms distant from the T_8-F cage, and it is unlikely that these would induce the ^{29}Si NMR signal observed at a chemical shift corresponding to a T_8-F cage. In addition, there is no evidence of the T^1 and/or T^2 signals around the ethoxy chemical shift that would be associated with such a reaction, and the T^0 signal is sharp, as would be expected for an unhydrolysed compound.

In contrast, work in our group using the analogous styryl-functionalised T_8, T_{10} and T_{12} systems has clearly demonstrated the formation of the corresponding oligomeric homopolymers in the presence of AIBN as initiator [14]. The reaction between styryl-functionalised T_8 (and T_{10}) POSS with mercaptopropyltriethoxysilane yielded the product of the expected thiol-ene click reaction in these systems [14], while the corresponding reaction with styryl-functionalised T_{12} POSS yielded a homopolymer. These results suggest that it is entirely reasonable to attribute the minor products observed during the AIBN-catalysed reaction of styryl-functionalised T_8-F with mercaptopropyltriethoxysilane to an oligomer formed by homo-condensation of adjacent styryl T_8-F molecules.

1.6 Formation of gels incorporating intact T_8-F silsesquioxane cages

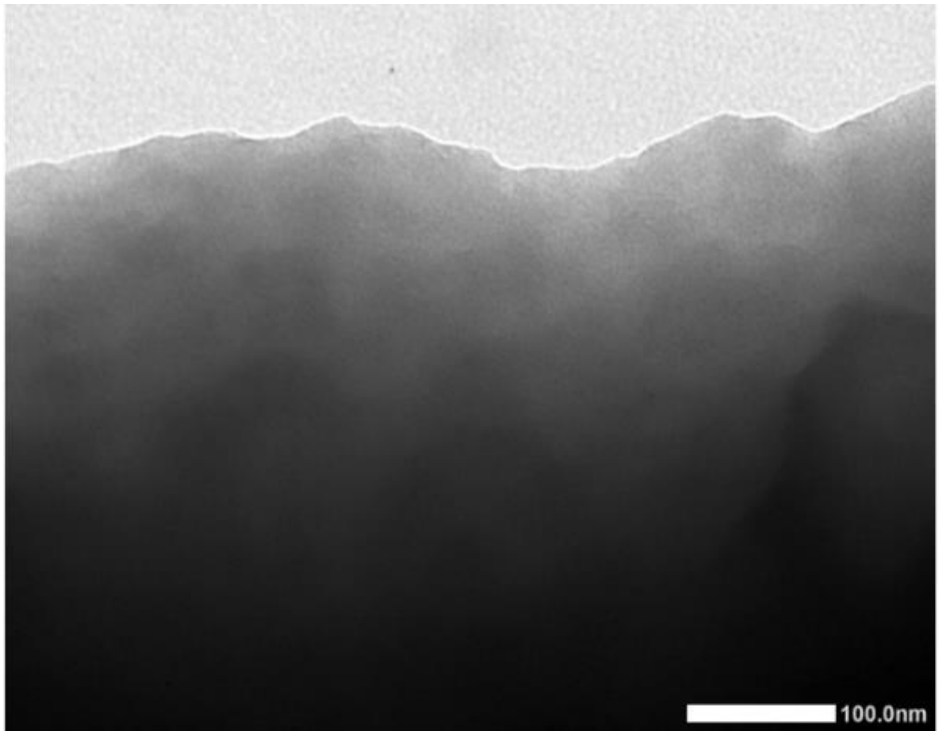

Fig. S11. TEM micrograph of the gel obtained from triethoxysilylated T_8-F cages.

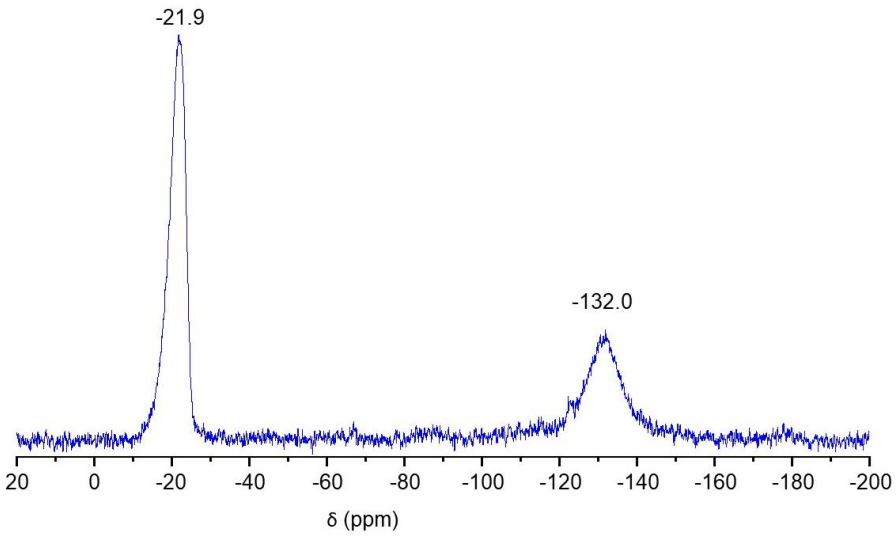

Fig. S12. ^{19}F SP-MAS solid state NMR spectrum of the T_8-F gel

References

1. M. Y. Lo, K. Ueno, H. Tanabe and A. Sellinger, *Chem. Rec.*, 2006, **6**, 157-168.
2. M. Laird, C. Totée, P. Gaveau, G. Silly, A. Van der Lee, C. Carcel, M. Unno, J. R. Bartlett and M. Wong Chi Man, *Dalton Trans.*, 2021, **50**, 81-89.
3. J. J. Levison and S. D. Robinson, *Journal of the Chemical Society A: Inorganic, Physical, and Theoretical Chemistry*, 1970, 2947-2954.
4. W. Caseri and P. S. Pregosin, *Organometallics*, 1988, **7**, 1373-1380.
5. S. Andre, F. Guida-Pietrasanta, A. Rousseau, B. Boutevin and G. Caporiccio, *Polymer*, 2001, **42**, 5505-5513.
6. J. H. Lamm, J. Horstmann, J. H. Nissen, J. H. Weddeling, B. Neumann, H. G. Stammler and N. W. Mitzel, *Eur. J. Inorg. Chem.*, 2014, **2014**, 4294-4301.
7. M. Laird, A. Van Der Lee, D. G. Dumitrescu, C. Carcel, A. Ouali, J. R. Bartlett, M. Unno and M. Wong Chi Man, *Organometallics*, 2020, **39**, 1896-1906.
8. D. Voisin, D. Flot, A. Van der Lee, O. J. Dautel and J. J. E. Moreau, *Crystengcomm*, 2017, **19**, 492-502.
9. H. J. Ben, X. K. Ren, B. Song, X. Li, Y. Feng, W. Jiang, E. Q. Chen, Z. Wang and S. Jiang, *J. Mater. Chem. C*, 2017, **5**, 2566-2576.
10. B. P. S. Chauhan, A. Sarkar, M. Chauhan and A. Roka, *Appl. Organomet. Chem.*, 2009, **23**, 385-390.
11. P. G. Taylor, A. R. Bassindale, Y. El Aziz, M. Pourny, R. Stevenson, M. B. Hursthouse and S. J. Coles, *Dalton Trans.*, 2012, **41**, 2048-2059.
12. G. S. Remya and C. H. Suresh, *Phys. Chem. Chem. Phys.*, 2016, **18**, 20615-20626.
13. M. Laird, N. Herrmann, N. Ramsahye, C. Totée, C. Carcel, M. Unno, J. R. Bartlett and M. Wong Chi Man, *Angew. Chem. Int. Ed.*, 2021, **60**, 3022-3027.
14. M. Laird, J. Yokoyama, C. Carcel, M. Unno, J. R. Bartlett and M. Wong Chi Man, *J Sol Gel Sci Technol*, 2020, **95**, 760-770.